

Geophysical Research Letters[®]

RESEARCH LETTER

10.1029/2023GL106577

Key Points:

- Long-term changes are detected in different aspects of the distribution of chlorophyll-a (not just the mean state)
- Oceanic chlorophyll-a high extremes are changing faster than chlorophyll-a mean globally during 1997–2022
- On a regional scale, chlorophyll-a extremes trends are predominant at high latitude (+), equatorial (−), and oligotrophic regions (−)

Supporting Information:

Supporting Information may be found in the online version of this article.

Correspondence to:

D. Zhai,
dzhai@ucsc.edu

Citation:

Zhai, D., Beaulieu, C., & Kudela, R. M. (2024). Long-term trends in the distribution of ocean chlorophyll. *Geophysical Research Letters*, 51, e2023GL106577. <https://doi.org/10.1029/2023GL106577>

Received 4 OCT 2023

Accepted 1 MAR 2024

Author Contributions:

Conceptualization: Dongran Zhai, Claudie Beaulieu
Data curation: Dongran Zhai
Formal analysis: Dongran Zhai, Claudie Beaulieu, Raphael M. Kudela
Funding acquisition: Dongran Zhai, Claudie Beaulieu
Methodology: Dongran Zhai, Claudie Beaulieu, Raphael M. Kudela
Project administration: Dongran Zhai, Claudie Beaulieu
Resources: Claudie Beaulieu
Supervision: Claudie Beaulieu
Visualization: Dongran Zhai
Writing – original draft: Dongran Zhai, Claudie Beaulieu

© 2024. The Authors.

This is an open access article under the terms of the [Creative Commons Attribution-NonCommercial-NoDerivs License](#), which permits use and distribution in any medium, provided the original work is properly cited, the use is non-commercial and no modifications or adaptations are made.

Long-Term Trends in the Distribution of Ocean Chlorophyll

Dongran Zhai¹ , Claudie Beaulieu¹ , and Raphael M. Kudela¹ 

¹University of California, Santa Cruz, Santa Cruz, CA, USA

Abstract The concentration of chlorophyll-a (CHL) is an important proxy for autotrophic biomass and primary production in the ocean. Quantifying trends and variability in CHL are essential to understanding how marine ecosystems are affected by climate change. Previous analyses have focused on assessing trends in CHL mean, but little is known about observed changes in CHL extremes and variance. Here we apply a quantile regression model to detect trends in CHL distribution over the period of 1997–2022 for several quantiles. We find that the magnitude of trends in upper quantiles of global CHL (>90th) are larger than those in lower quantiles (≤50th) and in the mean, suggesting a growing asymmetry in CHL distribution. On a regional scale, trends in different quantiles are statistically significant at high latitude, equatorial, and oligotrophic regions. Assessing changes in CHL distribution has potential to yield a more comprehensive understanding of climate change impacts on CHL.

Plain Language Summary The marine environment is essential to nature and society, as it provides food and other important services such as Earth's climate regulation and habitat for species. Marine primary productivity is increasingly stressed due to global climate change. Detecting the impact of climate change on primary producers should be a priority given their critical role in the climate system. Most studies focus on the impact of climate change by evaluating the mean state of primary productivity, but little is known about whether and how climate change is impacting variance and extremes. Here we assess changes in chlorophyll-a (CHL), which is an important proxy for primary production of marine ecosystems. We quantify long-term changes in different aspects of the CHL distribution (mean, variance, and extremes) using a quantile regression model. We find that CHL high extremes and variability are slightly intensified globally during the 26 years of observational record. Trends in regional scales, especially in high-latitude and North Atlantic Subtropical Gyre, show that CHL high extremes have been increasing since 1997. Our results suggest that more emphasis should be put into understanding the impact of climate change on the variance and extremes of primary productivity for climate change adaptation and mitigation.

1. Introduction

Global climate change is increasingly affecting marine ecosystems, altering the ocean's biological primary productivity. Based on coupled model projections, a global decline in primary productivity is expected due to changes in temperature, light, nutrients, and grazing (Bopp et al., 2013; Kwiatkowski et al., 2020), with potential repercussions on marine ecosystems (Laufkötter et al., 2015), fisheries (Free et al., 2019), and the global carbon cycle (Sarmiento et al., 2004). Marine phytoplankton contribute nearly half of the global primary productivity (Field et al., 1998). Consequently, detecting the impact of climate change on marine phytoplankton should be a priority given the critical role that primary productivity play in physical and biogeochemical interactions in the ocean.

Chlorophyll-a (CHL) is an essential climate variable and an important proxy for marine primary productivity (Bojinski et al., 2014; Hollmann et al., 2013). Satellite CHL offers high temporal and spatial resolution to support global and regional assessments of long-term changes in CHL (Bindoff et al., 2022; Blondeau-Patissier et al., 2014; McClain, 2009). To date, studies of long-term trends in CHL have focused on changes in the mean state (Boyce et al., 2010; Boyce et al., 2010; Gregg et al., 2005; Hammond et al., 2020; Henson et al., 2010; Henson et al., 2016; Mélin, 2016; Saulquin et al., 2013). Although assessing long-term trends in the mean is important for understanding how CHL is changing, this does not depict a complete portrait of changes. Assessing changes in variability and extremes may yield a more complete understanding of climate change impacts on CHL.

Ocean extremes and their impact on marine ecosystems have sparked a lot of attention and concern recently (Gruber et al., 2021). Marine heatwaves, low oxygen concentrations, and high acidity events are expected to

Writing – review & editing:

Dongran Zhai, Claudie Beaulieu, Raphael M. Kudela

intensify and occur more often, with impacts on organisms and ecosystems, further affecting ecosystem services and human welfare (Gruber et al., 2021). Compound extreme events, where two or more ocean extremes are happening synergistically (e.g., low oxygen and high temperature) are of particular concern as they can contribute to biological and ecological impacts in different ways (Burger et al., 2022; Gruber et al., 2021; Le Grix et al., 2021). Several studies have considered how the ocean's variance may be responding to climate change, including sea surface temperatures (Alexander et al., 2018), marine carbon dioxide (Landschützer et al., 2018), sea ice (Tareghian & Rasmussen, 2013), sea level (Barbosa, 2008), and phytoplankton biomass (Elsworth et al., 2022). A recent study showed that changes in variance are omnipresent in different aspects of Earth's climate and span physical and ecosystem variables, and tend to be more predominant in variables that are typically not normally distributed such as primary production (Rodgers et al., 2021). To our knowledge, there is no prior assessment of change in global CHL distribution over the observational period.

In this study, we provide a first assessment of changes in the whole CHL distribution, since other aspects of the CHL distribution (e.g., extremes) may be equally or even more important than the mean CHL. Our objective is to assess observed long-term trends in CHL distribution globally and regionally. Two multi-mission satellite products are utilized to expand the variety of results on global and regional scales and reduce the effect of the sensitivity of data sets. The impact of seasonality is also taken into account. We estimate long-term trends in multiple quantiles of a time series using quantile regression (QR), which together represent spatial and temporal changes in the distribution, including the tails representing extreme events (Cai & Reeve, 2013).

2. Data and Methodology

2.1. Data

We use two chlorophyll-a (mg/m^3) data products spanning 1997 to 2022. The first one is derived from the ESA's Ocean Color Climate Change Initiative (OC-CCI) project version 6.0 (Sathyendranath et al., 2019). This is a satellite multi-mission data product computed from merging the remote-sensing reflectance of a set of sensors, including Sea-viewing Wide Field-of-view Sensor (SeaWiFS), Moderate Resolution Imaging Spectroradiometer onboard the Aqua (MODIS-A), Medium Resolution Imaging Spectrometer (MERIS), Visible Infrared Imaging Radiometer Suite (VIIRS), and Ocean and Land Colour Instrument (OLCI). We use OC-CCI as the primary data set since it is deemed more suitable for climate assessments (Jackson et al., 2020). Potential inter-mission discontinuities are less pronounced in the OC-CCI data set, and it better compares with in situ observations than the GlobColour data set (Hammond et al., 2018; Jackson et al., 2021).

The second data set is derived from the GlobColour Project of the Copernicus Marine Environment Monitoring Service (CMEMS). This merged chlorophyll-a product is constructed by a combination of chlorophyll-a products directly computed for each sensor (SeaWiFS, MODIS-A, MERIS, VIIRS, and OLCI) (Garneron et al., 2019), which provides a “cloud-free” product by space-time interpolation. While the focus of our analysis is on the OC-CCI data set, we include additional analyses of GlobColour in the Supporting Information S1 as a measure of sensitivity.

Both data sets cover from September 1997 to December 2022 and are gridded at 4 km spatial resolution and monthly temporal resolutions. They have been regridded from a $1/24^\circ$ grid to a 1° grid by averaging within 1° boxes. Before fitting the QR model, the monthly data is deseasonalized in both data sets using an additive time series decomposition (assuming a constant seasonal cycle). We analyze these two data products at the global level, as well as regionally. Regions definitions are provided in Supporting Information S1 (Text S1).

2.2. Quantile Regression Model

To quantify changes in CHL distribution, we estimate trends in different distribution quantiles via QR (Koenker & Bassett, 1978). While assessing change in the mean of climate variables using ordinary least squares (OLS) provides extremely valuable information, it does not provide insight into changing extremes and how overall variability is related to time-varying events (Abbas et al., 2019). The main difference with OLS is that QR substitutes the conditional mean function in OLS for a conditional quantile function (Koenker & Bassett, 1978; Koenker & D'Orey, 1987). As such, instead of modeling the mean response in the regression model, QR models the response at a given quantile level. The QR model makes no assumptions about the distribution of the target variable and the residuals. Specifically, QR can identify opposite trends in statistical extremes (upper and lower)

that would remain hidden if focusing on means (Sankarasubramanian & Lall, 2003; Tareghian & Rasmusen, 2013). We use a QR model to assess trends of CHL in various quantile levels, where CHL observations at time t (in months) are represented by y_t ($t = 1, \dots, n$). We fit a model of the form:

$$y_\tau(t) = \alpha^\tau + \beta^\tau t, \quad (1)$$

where $y_\tau(t)$ is the response variable (i.e., CHL) for the conditional quantile τ , and parameters α^τ and β^τ denote the intercept and slope for a model of the τ th quantile of y_t , respectively. To estimate the parameters of the τ th quantile regression model, we minimize the tiled absolute value function:

$$f(\alpha^\tau, \beta^\tau) = \sum_{\{t|y_t < \hat{y}_\tau(t)\}} (1 - \tau)|y_t - \hat{y}_\tau(t)| + \sum_{\{t|y_t > \hat{y}_\tau(t)\}} \tau|y_t - \hat{y}_\tau(t)| \quad (2)$$

where $\hat{y}_\tau(t) = \hat{\alpha}^\tau + \hat{\beta}^\tau t$ represent the regression line (predicted values) for the τ th quantile. The absolute value of the difference between y_t and the corresponding τ th quantile $\hat{y}_\tau(t)$ is weighted by $(1 - \tau)$ if the observation is below the quantile line and by τ if y_t is above the line. The errors of the τ th quantile regression can be obtained such that $e_{\tau t} = y_t - \hat{y}_\tau(t)$.

We fit QR models at several quantile levels (5%, 10%, 50%, 90%, and 95% levels). As a comparison, OLS is also used here to fit trends in the mean CHL. The quantile regression model is implemented using the R package `quantreg` (Koenker et al., 2018).

2.3. Serially Correlated Residuals

Monthly chlorophyll-a concentration may exhibit serial autocorrelation in time series, which may bias trend detection if not taken into account (Beaulieu et al., 2013). Here we assume that residuals in CHL may follow a first-order autocorrelation (AR(1)) model. The quantile regression residuals at level τ , $e_{\tau t}$, are given by:

$$e_{\tau t} = \phi^\tau e_{\tau t-1} + \nu_{\tau t}, \quad (3)$$

where ϕ^τ is the first-order autocorrelation of residuals of the quantile regression at level τ and $\nu_{\tau t}$ denotes white noise errors.

In the presence of correlated errors QR estimates are less efficient and the inference is invalid (Huo et al., 2017; Koenker et al., 2017). To verify the presence of autocorrelation in the residuals of the QR, we test the following hypothesis:

$H_0: \phi^\tau = 0, H_1: \phi^\tau \neq 0$. We use a residual-based autocorrelation test, named the QF test (Huo et al., 2017). The test statistic is given by:

$$QF_n = \frac{\sum_{t=1}^n \hat{v}_{\tau t}^2 - \sum_{t=1}^n \hat{v}_{\tau t}^2}{\sum_{t=1}^n \hat{v}_{\tau t}^2 / (n - p - k)}, \quad (4)$$

where $\hat{v}_{\tau t}^2$ denotes the residuals from the AR(1) model fitted on the quantile residuals in Equation 3, under the alternative hypothesis (H_1), $\hat{v}_{\tau t}^2$ denotes the residuals under the null hypothesis (H_0) in which all parameters are estimated with no autocorrelation, n is the length of time series, p is the autocorrelation order (1), and k is the number of explanatory variables (1). The asymptotical distribution of the QF statistic is a chi-squared distribution with p degrees of freedom. More detailed information is presented in Huo et al. (2017).

If serial correlation is detected in the residuals from the QF test, we transform the time series by modifying the response variable (Cochrane & Orcutt, 1949):

$$y_t - \hat{\phi}^\tau y_{t-1} = \hat{\alpha}^\tau (1 - \hat{\phi}^\tau) + \hat{\beta}^\tau (t - \hat{\phi}^\tau (t - 1)) + \nu_{\tau t}, \quad (5)$$

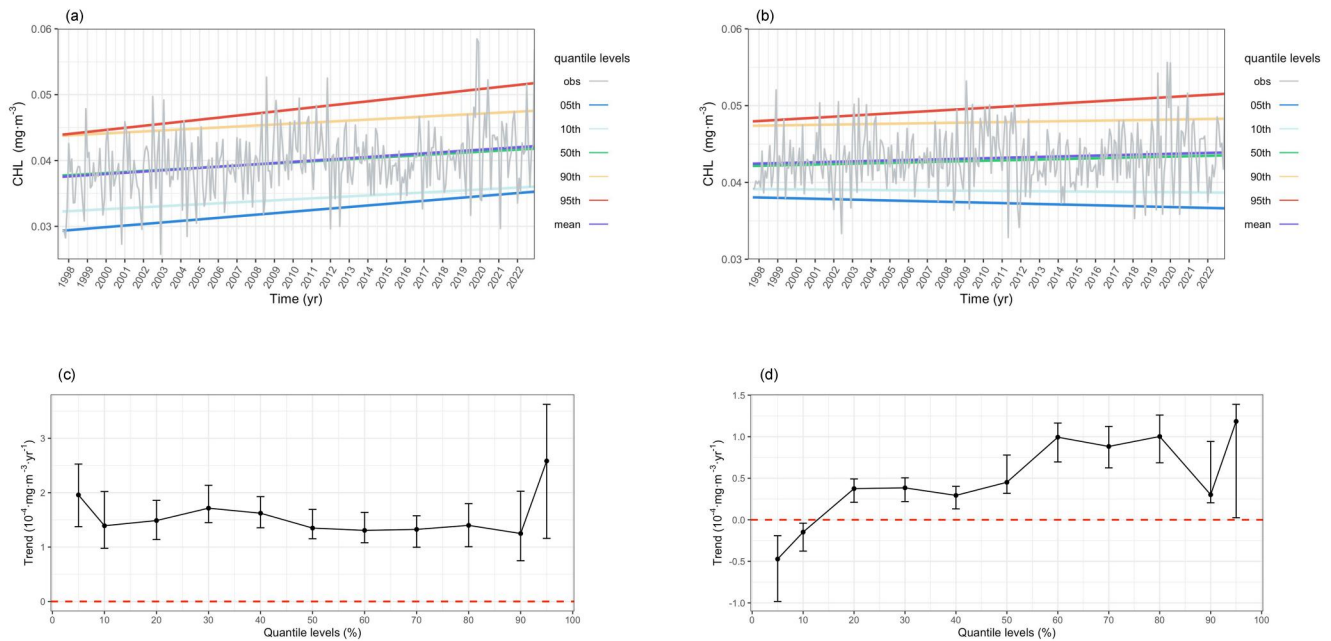


Figure 1. Time series of monthly global mean CHL from 1997 to 2022 with trends fitted in different quantile levels from (a) OC-CCI product and (b) GlobColour product. Trends in different quantile levels (5th to 95th levels) with 95% confidence intervals from (c) OC-CCI product and (d) GlobColour product. Trends were fitted to transformed data to remove autocorrelation.

Where $\hat{\alpha}^r$ and $\hat{\beta}^r$ are estimated from Equation 1. The autoregressive parameter $\hat{\phi}^r$ is estimated by first regressing the untransformed QR model and obtaining the residuals ϵ_t , then regressing ϵ_t on ϵ_{t-1} . Note that the first data point is lost in this process, and there are $n-1$ residual terms ν_{tt} after transformation. If the transformation is successful, the ν_{tt} should be white noise. To account for potential sensitivity to the choice of transformation method, we also use the Hildreth-Lu procedure (Hildreth & Lu, 1960). This procedure is also a transformation based on differencing as in Equation 5, but the Hildreth-Lu procedure offers a simultaneous estimation of the autocorrelation of the disturbances and the coefficients (Dufour et al., 1980). Results using Hildreth-Lu are included in Supporting Information S1 (Text S2 and Figure S1).

3. Results

3.1. Global Trends and Variability

On a global scale, trend estimates vary according to quantile levels (Figure 1). The magnitude of trend in the upper quantile of global CHL (95th) is larger than those in the middle and lower quantiles (<50th) (Figures 1a and 1b). As shown in Figures 1c and 1d, though the magnitude and uncertainty of global CHL trends differ by quantile level, most of the quantile levels show an increase in CHL. All trends are shown after removing serial correlation.

For the OC-CCI data product, all quantiles present a positive and significant trend (Figures 1a and 1c). The CHL trends in upper quantile (95th) are the steepest with a magnitude of $2.5 \times 10^{-4} \text{ mg m}^{-3} \text{ yr}^{-1}$, whereas the lower and middle quantiles show trends with smaller magnitudes. These features suggest a slight increase in the variance of global CHL given a more pronounced increase in the upper quantile than in lower quantiles, although trend uncertainty is also larger for the 95th quantile. A positive trend of $1.2 \times 10^{-4} \text{ mg m}^{-3} \text{ yr}^{-1}$ is detected by applying an OLS regression model that is almost identical to trends in median CHL (50th quantile). It indicates that the average and median global CHL are changing closely, and at a slightly lower pace than lower and upper extreme concentrations. The 95% confidence intervals in all quantile levels suggest the larger uncertainty (± 0.5 and $\pm 1.2 \times 10^{-4} \text{ mg m}^{-3} \text{ yr}^{-1}$) in the lower and upper quantiles, compared to middle quantiles with $\pm 0.2 \times 10^{-4} \text{ mg m}^{-3} \text{ yr}^{-1}$.

The trends and their variability in global CHL are similar for most quantiles in the GlobColour data product (Figures 1b and 1d). Although negative trends are detected in the 5th and 10th quantile levels, trends in upper and

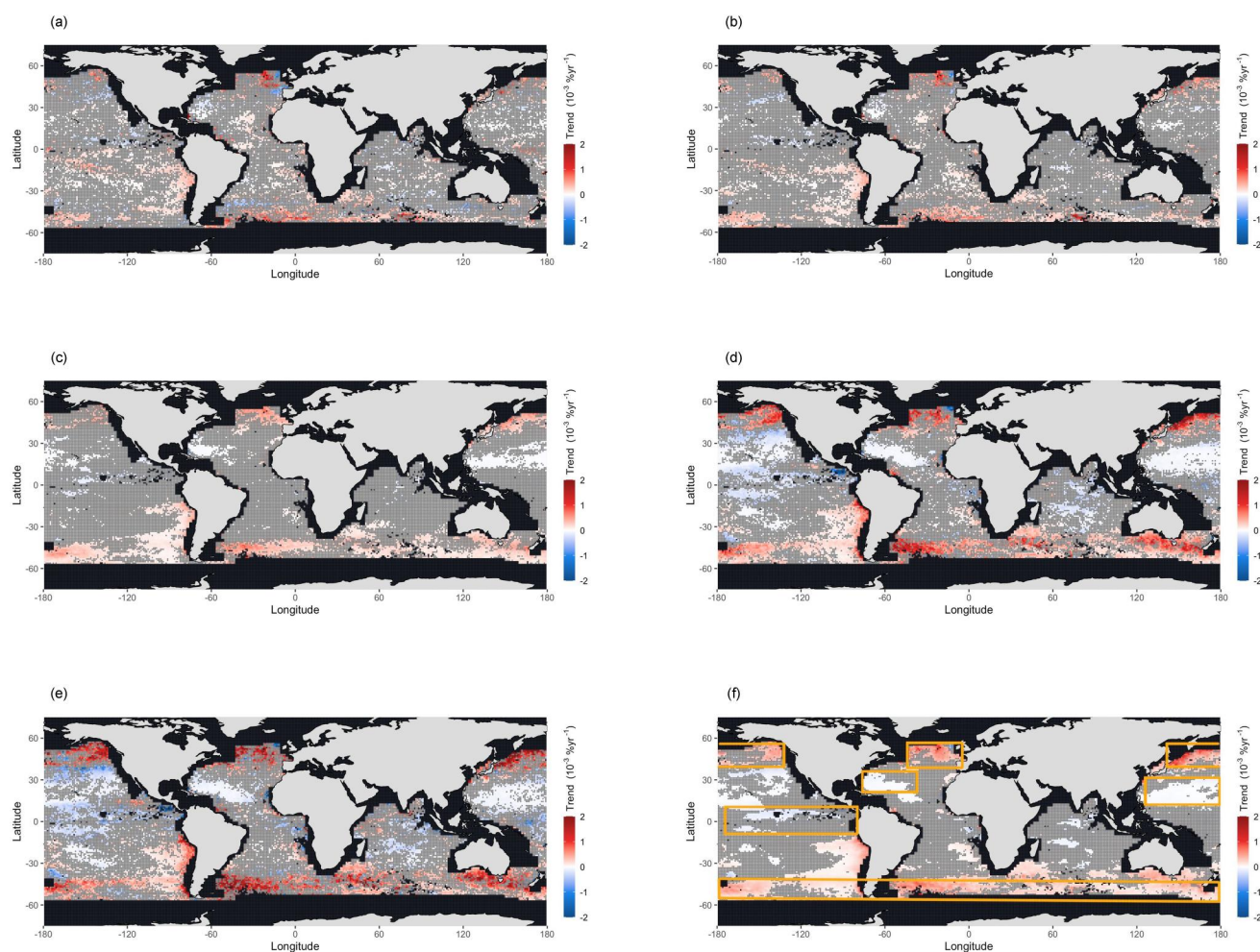


Figure 2. Maps of CHL trends from the OC-CCI data product during 1997–2022 in (a) 5th, (b) 10th, (c) 50th, (d) 90th, (e) 95th quantile levels, and (f) in CHL mean, respectively. Trends were fitted to transformed data to remove autocorrelation via the Cochrane-Orcutt procedure. The gray shadows are regions where trends are not significant at a 5% level.

middle quantile levels are positive. Again, upper quantile levels have a larger uncertainty (Figure 1d). A trend in CHL mean is $1 \times 10^{-4} \text{ mg m}^{-3} \text{ yr}^{-1}$ that is very similar to trends in median CHL ($0.5 \times 10^{-4} \text{ mg m}^{-3} \text{ yr}^{-1}$). The difference in trend sign between global CHL high and low imply an increasing variability over this period. This increase in variability is less pronounced in the OC-CCI data set, with the lower and upper quantiles having the same trend sign but different magnitudes (Figure 1a). The results are not sensitive to a log-transformation of CHL (Text S2 and Figure S2 in Supporting Information S1). Global trends in multiple quantile levels are slightly reduced under the assumption of changing seasonal cycle (Text S4, Figures S9, and S10 in Supporting Information S1).

3.2. Regional Trends

Trends estimated in each grid cell are presented in Figure 2. After a preliminary analysis, the presence of autocorrelation was detected in most areas of the ocean (Figure S3 in Supporting Information S1). As such, a Cochrane-Orcutt transformation was applied to remove autocorrelation from the data. It must be noted that this transformation does not remove the trend signal, but only sieve the autocorrelation. As a comparison, a different transformation procedure was used to remove autocorrelation from the data, the Hildreth-Lu method (Figure S1 in Supporting Information S1). Results are consistent with the Cochrane-Orcutt transformation (Text S2 and Figure S1 in Supporting Information S1), suggesting that the results are robust to the choice of transformation approach.

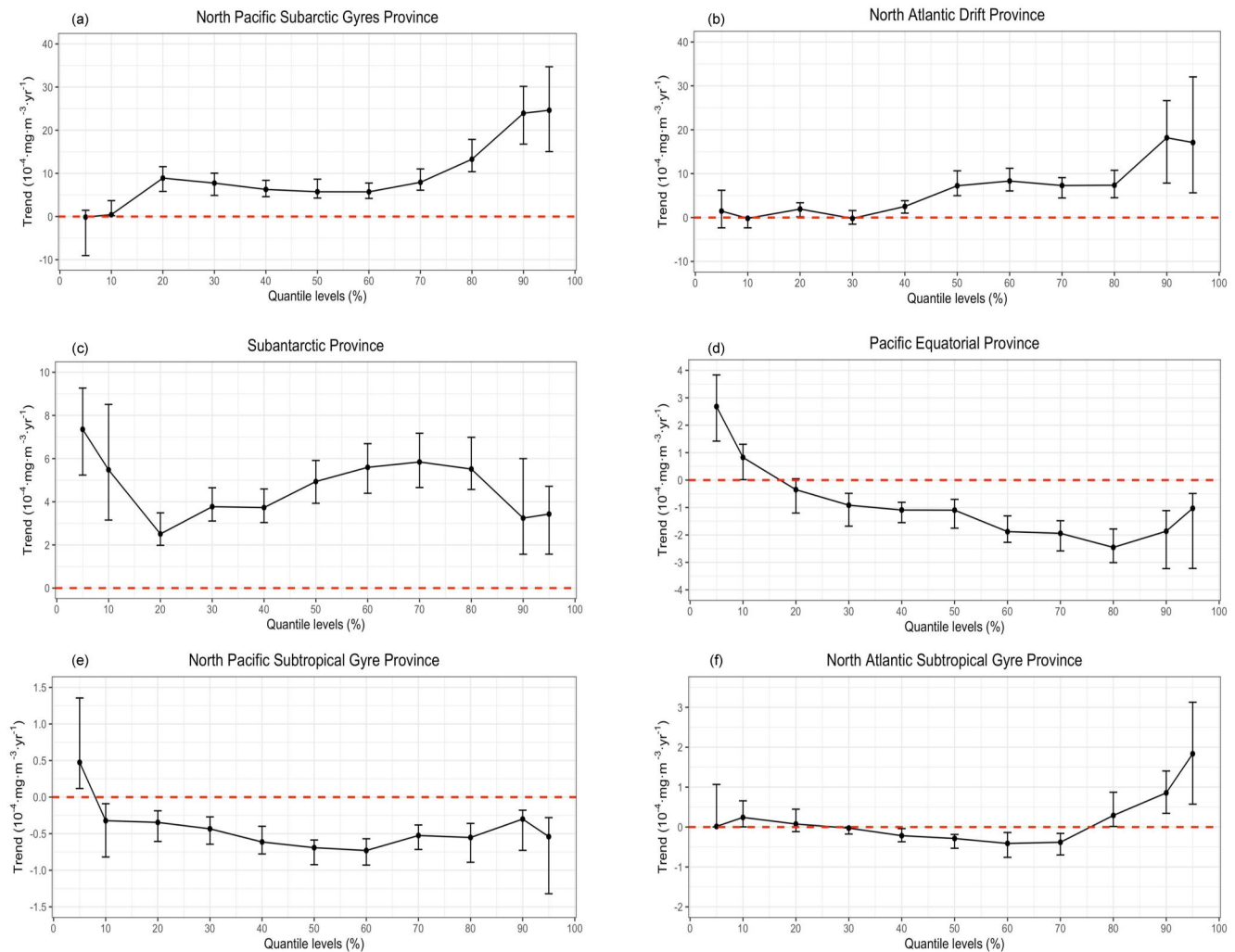


Figure 3. Regional CHL trends in OC-CCI data product in different quantile levels in regions, (a) North Pacific Subarctic Gyre Province, (b) North Atlantic Drift Province, (c) Subantarctic Province, (d) Pacific Equatorial Province, (e) North Pacific Subtropical Gyre Province, and (f) North Atlantic Subtropical Gyre Province. The 95% confidence intervals for each regression are represented by the vertical lines. The red horizontal dashed line is zero.

At the regional scale, trends in lower quantiles are more scattered (Figures 2a and 2b), and patterns become more apparent in the median and larger quantiles (Figures 2c–2e). Overall, regions with significant trends in the upper quantiles are mainly located at high latitudes (+), in equatorial (–), and oligotrophic regions (–) (Figures 2d and 2e). A few regions emerge with consistent patterns of change in North Pacific Subarctic Province, North Atlantic Drift Province, Subantarctic Province, Pacific Equatorial Province, North Pacific Subtropical Gyre, and North Atlantic Subtropical Gyre, and are highlighted in Figure 2f. The regions are divided as defined by Longhurst (1995) (see Text S1 in Supporting Information S1).

In Figure 3, we further look into the regions with significant trends identified above. We averaged grid cells in these regions and estimated trends with their respective confidence intervals. Trends in different quantiles may vary in magnitude and sign, suggesting that the shape of the CHL distribution is varies on a regional scale. Positive trends dominate in the North Pacific Subarctic Province, North Atlantic Drift Province, and Subantarctic Province (Figures 3a–3c). Trends in Subantarctic Province are positive in all quantile levels, while the North Pacific Subarctic Province and North Atlantic Drift Province exhibit similar patterns whereby trends in lower quantiles are not significant and median and upper quantiles are significant and positive. In these three regions, trends detected in different quantiles are consistent with an increasing variability over the observational record. In low nutrient regions, namely the Pacific Equatorial Province and North Pacific Subtropical Gyre, trends in the lower quantiles are significantly increasing even if negative trends are observed in the mean/median (Figures 3d

and 3e). It might indicate that CHL low extremes become less frequent during the recording period. Among these regions, Pacific Equatorial Province and North Pacific Subtropical Gyre present consistent trends with an overall decrease in variability. The North Atlantic Subtropical Gyre exhibits decreasing trends in middle quantile levels and increasing trends at upper quantiles, suggesting a slightly increasing variance over time. Trend estimates obtained by the OLS model closely follow those for the median in all of the regions (see Figure S4 in Supporting Information S1).

Most regions show increasing variability in CHL except Pacific Equatorial and North Pacific Subtropical Gyre Province. The large variance of CHL relates to climate seasonality and dominates at high latitudes, sub-polar, and coastal waters. December, January, and February (DJF) and June, July, and August (JJA) are two seasons that are commonly used to analyze ocean phytoplankton blooms because they represent contrasting environmental conditions that affect the growth and distribution of phytoplankton in the ocean. The impact of regional seasonality is shown in Supporting Information S1 (Text S2 and Figure S5).

We also include results obtained on the GlobColour data set in these regions to assess the sensitivity of our findings to the choice of the data set in Text S3 in Supporting Information S1. In most regions, trends detected in different quantiles are consistent except for the North Atlantic Drift province and the North Pacific Subtropical Gyre Province (Figures S6–S8 in Supporting Information S1). The variability is increasing in most regions (except Subantarctic region) under the assumption of changing seasonal cycle (Text S4 and Figure S11 in Supporting Information S1).

4. Discussion and Conclusion

In this study, we provide a first assessment of changes in CHL distribution in the global ocean over the 1997–2022 period. At the global scale, our results suggest that different quantiles are changing at different rates, with CHL high extremes changing faster than the rest of the distribution. This difference in pace results in an overall slight increase in CHL variability. At the regional scale, CHL high extremes are increasing at high latitudes and decreasing in equatorial and oligotrophic regions. These changes are consistent with Earth System Models projections whereby high latitude oceans are light-limited while equatorial and oligotrophic regions are limited by nutrients (Doney, 2006; Doney et al., 2012; Kwiatkowski et al., 2020). Furthermore, we show that changes at high latitudes are more pronounced during DJF season, while changes in equatorial regions dominate during JJA. This may be due to climate processes like El Niño–Southern Oscillation (ENSO) that tend to start during JJA in equatorial regions.

In a study focusing on analyzing phytoplankton carbon biomass in an Earth System Model large ensemble, Elsworth et al. (2022) identified decreasing variability of global phytoplankton variance from 1920 to 2100. Our results do not show an overall decreased variability in CHL. This difference may be due to the differing periods of analysis. Indeed, our analysis focuses on the period 1997–2022, and changes detected over that period may be more indicative of decadal variability rather than long-term impact of climate change over 1920–2100. Another explanation could be that the two studies are analyzing different variables. While previous studies have discussed the correlation between the spatial distribution of CHL (used in this study) and phytoplankton carbon biomass (Kostadinov et al., 2016; Martínez-Vicente et al., 2017), those variables tend to decouple especially in subtropical regions (Barbieux et al., 2018). Future work should focus on analyzing CHL extremes and variability in models to assess whether long-term changes in CHL variability and extremes are consistent with observations, in order to better understand their drivers and anticipate future changes.

Regional trends differ from those at the global scale with mixed signs and larger magnitudes. Regions with significant trends in upper quantiles include the North Pacific Subarctic Province (+), North Atlantic Drift Province (+), Subantarctic Province (+), Pacific Equatorial Province (−), North Pacific Subtropical Gyre (−), and North Atlantic Subtropical Gyre (−), as shown in Figure 2f. Regional changes in upper quantiles described above also correspond to changes in CHL variability with increase in the North Pacific Subarctic Province, North Atlantic Drift Province, and Subantarctic Provinces, and declining variability in Pacific Equatorial and North Pacific Subtropical Gyre Province. Those regions are characterized by noticeable ecological and biogeochemical seasonal variability that is closely related to strong annual cycles in light, nutrients, temperature, wind force, and zooplankton grazing at surface (Elsworth et al., 2022; Henson et al., 2010). At the regional scale, large-scale climate patterns such as El Niño Southern Oscillation (ENSO), Pacific Decadal Oscillation (PDO), and North Atlantic Oscillation (NAO) are known drivers of CHL trends and variability (Corno et al., 2007; Gao et al., 2020;

Kang et al., 2017; Le Grix et al., 2021; L. Zhai et al., 2013). In the North Pacific Subarctic Gyres and North Atlantic Drift Provinces, warming over the last two decades has resulted in more phytoplankton blooming (Dunstan et al., 2018). Our results showing that CHL high extremes are becoming more frequent are consistent with Dunstan et al. (2018) and Kahru and Mitchell (2008) findings. Changes in the North Atlantic Drift region are more pronounced than the North Pacific Subarctic Gyre, also consistent with previous analysis on phytoplankton blooms (Westberry et al., 2016).

As for the Southern hemisphere, seasonal variation in the location of transition zones between subpolar and subtropical gyres coincide with increasing CHL variance (Dunstan et al., 2018). This phenomenon may indicate that the increasing seasonal variance plays a role in the CHL distribution changes detected here (Thomalla et al., 2023). Trends in Subantarctic Province are significantly positive in all quantile levels. A possible explanation is that though iron limitation controls the Southern Ocean, sea surface warming could still be an important driver on seasonal phytoplankton blooms in this region instead of light or nutrients (Laufkötter et al., 2015; Moore et al., 2013), resulting in positive and similar magnitude changes in CHL distribution and their variability over the observational period.

Some limitations in this study may impact the validity of our results. First, the shortness of the record may impact our results, as we use observations over a period that is slightly shorter (26 years) than the recommended 30 years for assessing climate change impacts (WMO, 2018). More specifically, satellite ocean color data sets require multiple decades to distinguish long-term climate-related trends from natural variability (Beaulieu et al., 2013; Bindoff et al., 2022; Henson et al., 2010), although exact detection timescales vary depending on regional interannual and decadal variability and magnitude of trends (Henson et al., 2010). That said, previous studies aimed at estimating timescales of trend detection in ocean CHL (Beaulieu et al., 2013; Henson et al., 2010) focused on mean changes in CHL, not variability and extremes, and these detection times may be different here. Recent studies also suggested that long-term trends in satellite ocean color may be detectable faster in reflectance rather than CHL (Cael et al., 2023; Dutkiewicz et al., 2019). Assessing whether similar patterns can be detected in reflectance observations should be the focus of a future study.

Second, merged time series of multimission products used here are susceptible to biases, which may impact the CHL trends detected (Hammond et al., 2018; Mélin, 2016; Mélin et al., 2017; Saulquin et al., 2013). GlobColour merges multi-sensor CHL with a specific flagging, but is not explicitly bias-corrected (Garnesson et al., 2019; Maritorena et al., 2010; Yu et al., 2023). For the OC-CCI product, multi-sensors reflectance is merged before CHL derivation, which results in a more constrained approach (Sathyendranath et al., 2017). As a result, long-term CHL trends detected in OC-CCI and GlobColour products differ in some regions (e.g., North Pacific Subarctic Gyre and North Atlantic Drift Provinces). By utilizing the two data sets, we reduce the sensitivity of our results to the choice of data sets and bias correction algorithms, but we cannot entirely eliminate the possibility of bias in trends detected introduced from using multiple mission data products. We focus on the OC-CCI data set as previous work showed that this data product is more suited for climate studies (Jackson et al., 2020), provides better match-ups with in situ observations (Jackson et al., 2021) and potential discontinuities due to merging data sets are less pronounced in the OC-CCI data product (Hammond et al., 2018). In addition to bias arising from merging data sets, there may be additional uncertainty introduced by the aging optical components. The aging optical components reduce the responsivity of radiometers through time (Zibordi et al., 2019).

Third, few studies have used satellite-derived CHL data sets to analyze extremes (Le Grix et al., 2021; Woolway et al., 2021). Bias due to high solar zenith angles, clouds, and aerosols may affect the data (Gregg et al., 2009; Le Grix et al., 2021). Low sampling rates of CHL extremes may also affect our results. The majority of the surface ocean is characterized by low CHL levels in the Oligotrophic area, whereas high CHL levels are only present in a small portion (~1%) primarily located in coastal zones (Sathyendranath et al., 2019; Van Oostende et al., 2018). Insufficient data in CHL extremes corresponding to lower and upper quantile levels result in higher uncertainties (larger confidence intervals) for CHL trends.

Finally, we made assumptions when fitting the statistical model that may influence the results. We assume that trends in different quantiles are linear, following previous studies (Boyce et al., 2010; Boyce et al., 2010; Gregg et al., 2005; Hammond et al., 2020; Henson et al., 2010, 2016; Mélin, 2016; Saulquin et al., 2013). More complex time dependence such as nonlinear trends or abrupt changes were not assessed as linear trends can provide a first-order approximation to long-term changes and avoid over-fitting the data. Furthermore, the period of observations

is quite short, so there is a risk of overfitting with more complex time dependence. A constant seasonal pattern is assumed in our study, though some studies have shown that the CHL seasonal cycle might vary over time (Henson et al., 2013; Vantrepotte & Mélin, 2009). A changing seasonal cycle over the period of observation may bias trends detected here. The magnitude of trend reduces slightly after removing a changing seasonal cycle, but in general the sign of trends remains the same and does not affect our conclusions (Figures S9–S11 in Supporting Information S1). There is one exception in the Subarctic Ocean, where trends in quantiles change from $1.9 \times 10^{-4} \text{ mg m}^{-3} \text{ yr}^{-1}$ to $6 \times 10^{-4} \text{ mg m}^{-3} \text{ yr}^{-1}$ when assuming a changing seasonal cycle, implying an increasing variability instead of decreasing variability under a constant seasonal cycle assumption. Most regions have increasing variability, whereas variability in Subantarctic province has decreasing variability with a changing seasonal cycle. Quantile regression models used here assume independent errors. To deal with the presence of autocorrelation, we used pre-whitening methods. These approaches help reduce the risk of a false detection (i.e., detecting a trend when there is none), but are also associated with a reduced power of detection (Bayazit & Önöz, 2007). As such, significant trends may not be detected. Results may also differ based on the pre-whitening approach used. Here, we reduced this problem by using two different pre-whitening approaches, Cochrane-Orcutt and Hildreth-Lu procedures, and showed our results were not sensitive to the choice of pre-whitening method (see Supporting Information S1).

To our knowledge, this is the first study assessing long-term changes in CHL distribution on a global scale, as opposed to focusing entirely on mean CHL. More information related to climate variables such as seasonal changes and their variability, as well as extreme conditions, are revealed by assessing trends in all quantile levels of the CHL distribution. We conclude that over the satellite record, trends in CHL extremes are more pronounced than those in the mean CHL. Henson et al. (2010) concluded that the current length of observation recording is insufficient to identify a climate change trend in mean CHL and suggested that a time series of approximately 40 years is needed to separate a global warming trend from natural variability. Our results show that trends in CHL high extremes tend to have larger magnitudes and uncertainties than trends in the mean, both of which may impact detection times. By considering the whole distribution (not just the mean), we may be able to detect climate change-related trends faster and more holistically, and better understand the effects of anthropogenic forcing on marine ecosystems, which will enable us to make more effective decisions concerning socioeconomic systems that are affected by climate change. Future work should focus on quantifying detection times in different aspects of CHL distribution to develop the ability to formally detect the impact of climate change in marine ecosystems as soon as possible.

Data Availability Statement

The OC-CCI data can be found on the open portal of ESA's climate office (Sathyendranath et al., 2021). The GlobColour data can be found on the GlobColour Project of Copernicus program (CMEMS, 2019). The R code used to produce the initial data set, statistically analyze the quantile regression model, and reproduce the figures of the manuscript is publicly available (D. Zhai, 2023).

Acknowledgments

We would like to thank the Ocean-Colour Climate Change Initiative and the GlobColour Project for making their data publicly available. DZ acknowledges financial support from the program of the China Scholarship Council No. 20200801001. CB thanks National Science Foundation Grant AGS-2143550 for partial support. RK thanks NASA Grant 80NSSC21K165 for partial support.

References

- Abbas, S. A., Xuan, Y., & Song, X. (2019). Quantile regression based methods for investigating rainfall trends associated with flooding and drought conditions. *Water Resources Management*, 33(12), 4249–4264. <https://doi.org/10.1007/s11269-019-02362-0>
- Alexander, M. A., Scott, J. D., Friedland, K. D., Mills, K. E., Nye, J. A., Pershing, A. J., & Thomas, A. C. (2018). Projected sea surface temperatures over the 21st century: Changes in the mean, variability and extremes for large marine ecosystem regions of northern oceans. *Elementa: Science of the Anthropocene*, 6. <https://doi.org/10.1525/elementa.191>
- Barbieux, M., Uitz, J., Bricaud, A., Organelli, E., Poteau, A., Schmechtig, C., et al. (2018). Assessing the variability in the relationship between the particulate backscattering coefficient and the chlorophyll a concentration from a global biogeochemical-Argo database. *Journal of Geophysical Research: Oceans*, 123(2), 1229–1250. <https://doi.org/10.1002/2017jc013030>
- Barbosa, S. M. (2008). Quantile trends in Baltic Sea level. *Geophysical Research Letters*, 35(22), L22704. <https://doi.org/10.1029/2008gl035182>
- Bayazit, M., & Önöz, B. (2007). To prewhiten or not to prewhiten in trend analysis? *Hydrological Sciences Journal*, 52(4), 611–624. <https://doi.org/10.1623/hysj.52.4.611>
- Beaulieu, C., Henson, S. A., Sarmiento, J. L., Dunne, J. P., Doney, S. C., Rykaczewski, R. R., & Bopp, L. (2013). Factors challenging our ability to detect long-term trends in ocean chlorophyll. *Biogeosciences*, 10(4), 2711–2724. <https://doi.org/10.5194/bg-10-2711-2013>
- Bindoff, N., Cheung, W., Kairo, J., Aristegui, J., Guinder, V., Hallberg, R., et al. (2022). Changing ocean, marine ecosystems, and dependent communities. In *The ocean and cryosphere in a changing climate: Special report of the intergovernmental panel on climate change* (pp. 447–587). Cambridge University Press. <https://doi.org/10.1017/9781009157964.007>
- Blondeau-Patissier, D., Gower, J. F., Dekker, A. G., Phinn, S. R., & Brando, V. E. (2014). A review of ocean color remote sensing methods and statistical techniques for the detection, mapping and analysis of phytoplankton blooms in coastal and open oceans. *Progress in Oceanography*, 123, 123–144. <https://doi.org/10.1016/j.pocan.2013.12.008>

- Bojinski, S., Verstraete, M., Peterson, T. C., Richter, C., Simmons, A., & Zemp, M. (2014). The concept of essential climate variables in support of climate research, applications, and policy. *Bulletin of the American Meteorological Society*, 95(9), 1431–1443. <https://doi.org/10.1175/bams-d-13-00047.1>
- Bopp, L., Resplandy, L., Orr, J. C., Doney, S. C., Dunne, J. P., Gehlen, M., et al. (2013). Multiple stressors of ocean ecosystems in the 21st century: Projections with CMIP5 models. *Biogeosciences*, 10(10), 6225–6245. <https://doi.org/10.5194/bg-10-6225-2013>
- Boyce, D. G., Lewis, M. R., & Worm, B. (2010). Global phytoplankton decline over the past century. *Nature*, 466(7306), 591–596. <https://doi.org/10.1038/nature09268>
- Burger, F. A., Terhaar, J., & Frölicher, T. L. (2022). Compound marine heatwaves and ocean acidity extremes. *Nature Communications*, 13(1), 4722. <https://doi.org/10.1038/s41467-022-32120-7>
- Cael, B., Bisson, K., Boss, E., Dutkiewicz, S., & Henson, S. (2023). Global climate-change trends detected in indicators of ocean ecology. *Nature*, 619(7970), 1–4. <https://doi.org/10.1038/s41586-023-06321-z>
- Cai, Y., & Reeve, D. E. (2013). Extreme value prediction via a quantile function model. *Coastal Engineering*, 77, 91–98. <https://doi.org/10.1016/j.coastaleng.2013.02.003>
- CMEMS. (2019). Global ocean colour bio-geo-chemical I4 from satellite observations (1997–ongoing) [Dataset]. *Marine Data Store (MDS)*. <https://doi.org/10.48670/moi-00281>
- Cochrane, D., & Orcutt, G. H. (1949). Application of least squares regression to relationships containing auto-correlated error terms. *Journal of the American Statistical Association*, 44(245), 32–61. <https://doi.org/10.1080/01621459.1949.10483290>
- Corno, G., Karl, D. M., Church, M. J., Letelier, R. M., Lukas, R., Bidigare, R. R., & Abbott, M. R. (2007). Impact of climate forcing on ecosystem processes in the north pacific subtropical gyre. *Journal of Geophysical Research*, 112(C4), C04021. <https://doi.org/10.1029/2006jc003730>
- Doney, S. C. (2006). Plankton in a warmer world. *Nature*, 444(7120), 695–696. <https://doi.org/10.1038/444695a>
- Doney, S. C., Ruckelshaus, M., Emmett Duffy, J., Barry, J. P., Chan, F., English, C. A., et al. (2012). Climate change impacts on marine ecosystems. *Annual Review of Marine Science*, 4(1), 11–37. <https://doi.org/10.1146/annurev-marine-041911-111611>
- Dufour, J.-M., Gaudry, M. J., & Liem, T. C. (1980). The cochrane-orcutt procedure numerical examples of multiple admissible minima. *Economics Letters*, 6(1), 43–48. [https://doi.org/10.1016/0165-1765\(80\)90055-5](https://doi.org/10.1016/0165-1765(80)90055-5)
- Dunstan, P. K., Foster, S. D., King, E., Risbey, J., O’Kane, T. J., Monselesan, D., et al. (2018). Global patterns of change and variation in sea surface temperature and chlorophyll a. *Scientific Reports*, 8(1), 14624. <https://doi.org/10.1038/s41598-018-33057-y>
- Dutkiewicz, S., Hickman, A. E., Jahn, O., Henson, S. A., Beaulieu, C., & Monier, E. (2019). Ocean colour signature of climate change. *Nature Communications*, 10(1), 578. <https://doi.org/10.1038/s41467-019-08457-x>
- Elsworth, G. W., Lovenduski, N. S., Krumhardt, K. M., Marchitto, T. M., & Schlunegger, S. (2022). Anthropogenic climate change drives non-stationary phytoplankton variance. *EGU sphere*, 1–21.
- Field, C. B., Behrenfeld, M. J., Randerson, J. T., & Falkowski, P. (1998). Primary production of the biosphere: Integrating terrestrial and oceanic components. *Science*, 281(5374), 237–240. <https://doi.org/10.1126/science.281.5374.237>
- Free, C. M., Thorson, J. T., Pinsky, M. L., Oken, K. L., Wiedenmann, J., & Jensen, O. P. (2019). Impacts of historical warming on marine fisheries production. *Science*, 363(6430), 979–983. <https://doi.org/10.1126/science.aau1758>
- Gao, N., Ma, Y., Zhao, M., Zhang, L., Zhan, H., Cai, S., & He, Q. (2020). Quantile analysis of long-term trends of near-surface chlorophyll-a in the Pearl River plume. *Water*, 12(6), 1662. <https://doi.org/10.3390/w12061662>
- Garnesson, P., Mangin, A., Fanton d’Andon, O., Demaria, J., & Bretagnon, M. (2019). The CMEMS GlobColour chlorophyll a product based on satellite observation: Multi-sensor merging and flagging strategies. *Ocean Science*, 15(3), 819–830. <https://doi.org/10.5194/os-15-819-2019>
- Gregg, W. W., Casey, N. W., & McClain, C. R. (2005). Recent trends in global ocean chlorophyll. *Geophysical Research Letters*, 32(3), L03606. <https://doi.org/10.1029/2004gl021808>
- Gregg, W. W., Casey, N. W., O’Reilly, J. E., & Esaias, W. E. (2009). An empirical approach to ocean color data: Reducing bias and the need for post-launch radiometric re-calibration. *Remote Sensing of Environment*, 113(8), 1598–1612. <https://doi.org/10.1016/j.rse.2009.03.005>
- Gruber, N., Boyd, P. W., Frölicher, T. L., & Vogt, M. (2021). Biogeochemical extremes and compound events in the ocean. *Nature*, 600(7889), 395–407. <https://doi.org/10.1038/s41586-021-03981-7>
- Hammond, M. L., Beaulieu, C., Henson, S. A., & Sahu, S. K. (2018). Assessing the presence of discontinuities in the ocean color satellite record and their effects on chlorophyll trends and their uncertainties. *Geophysical Research Letters*, 45(15), 7654–7662. <https://doi.org/10.1029/2017gl076928>
- Hammond, M. L., Beaulieu, C., Henson, S. A., & Sahu, S. K. (2020). Regional surface chlorophyll trends and uncertainties in the global ocean. *Scientific Reports*, 10(1), 15273. <https://doi.org/10.1038/s41598-020-72073-9>
- Henson, S. A., Beaulieu, C., & Lampitt, R. (2016). Observing climate change trends in ocean biogeochemistry: When and where. *Global Change Biology*, 22(4), 1561–1571. <https://doi.org/10.1111/gcb.13152>
- Henson, S. A., Cole, H., Beaulieu, C., & Yool, A. (2013). The impact of global warming on seasonality of ocean primary production. *Biogeosciences*, 10(6), 4357–4369. <https://doi.org/10.5194/bg-10-4357-2013>
- Henson, S. A., Sarmiento, J. L., Dunne, J. P., Bopp, L., Lima, I., Doney, S. C., et al. (2010). Detection of anthropogenic climate change in satellite records of ocean chlorophyll and productivity. *Biogeosciences*, 7(2), 621–640. <https://doi.org/10.5194/bg-7-621-2010>
- Hildreth, C., & Lu, J. (1960). *Demand relations with autocorrelated disturbances*. Technical Bulletin. Michigan State University Agricultural Experiment Station.
- Hollmann, R., Merchant, C. J., Saunders, R., Downy, C., Buchwitz, M., Cazenave, A., et al. (2013). The ESA climate change initiative: Satellite data records for essential climate variables. *Bulletin of the American Meteorological Society*, 94(10), 1541–1552. <https://doi.org/10.1175/bams-d-11-00254.1>
- Huo, L., Kim, T.-H., Kim, Y., & Lee, D. J. (2017). A residual-based test for autocorrelation in quantile regression models. *Journal of Statistical Computation and Simulation*, 87(7), 1305–1322. <https://doi.org/10.1080/00949655.2016.1262371>
- Jackson, Volpe, G., Sathyendranat, S., & Groom, S. (2020). *ESA Ocean colour climate change initiative—Phase 3 product user guide for v5.0 dataset* (pp. 1–50). ESA.
- Jackson, Volpe, G., Sathyendranat, S., & Groom, S. (2021). *ESA Ocean colour climate change initiative—Phase 3 product validation and inter-comparison report* (Vol. 4, pp. 1–17). Plymouth Marine Laboratory.
- Kahru, M., & Mitchell, B. G. (2008). Ocean color reveals increased blooms in various parts of the world. *Eos, Transactions American Geophysical Union*, 89(18), 170. <https://doi.org/10.1029/2008eo180002>
- Kang, X., Zhang, R.-H., Gao, C., & Zhu, J. (2017). An improved ENSO simulation by representing chlorophyll-induced climate feedback in the NCAR community earth system model. *Scientific Reports*, 7(1), 17123. <https://doi.org/10.1038/s41598-017-17390-2>
- Koenker, R., & Bassett, G., Jr. (1978). Regression quantiles. *Econometrica: Journal of the Econometric Society*, 46(1), 33–50. <https://doi.org/10.2307/1913643>

- Koenker, R., Chernozhukov, V., He, X., & Peng, L. (2017). *Handbook of quantile regression*. CRC Press.
- Koenker, R., & D'Orey, V. (1987). Computing regression quantiles, applied statistics.
- Koenker, R., Portnoy, S., Ng, P. T., Zeileis, A., Grosjean, P., & Ripley, B. D. (2018). *Package "quantreg"*. Cran R-project. org.
- Kostadinov, T. S., Milutinović, S., Marinov, I., & Cabré, A. (2016). Carbon-based phytoplankton size classes retrieved via ocean color estimates of the particle size distribution. *Ocean Science*, 12(2), 561–575. <https://doi.org/10.5194/os-12-561-2016>
- Kwiatkowski, L., Torres, O., Bopp, L., Aumont, O., Chamberlain, M., Christian, J. R., et al. (2020). Twenty-first century ocean warming, acidification, deoxygenation, and upper-ocean nutrient and primary production decline from CMIP6 model projections. *Biogeosciences*, 17(13), 3439–3470. <https://doi.org/10.5194/bg-17-3439-2020>
- Landschützer, P., Gruber, N., Bakker, D. C., Stemmler, I., & Six, K. D. (2018). Strengthening seasonal marine CO₂ variations due to increasing atmospheric CO₂. *Nature Climate Change*, 8(2), 146–150. <https://doi.org/10.1038/s41558-017-0057-x>
- Laufkötter, C., Vogt, M., Gruber, N., Aita-Noguchi, M., Aumont, O., Bopp, L., et al. (2015). Drivers and uncertainties of future global marine primary production in marine ecosystem models. *Biogeosciences*, 12(23), 6955–6984. <https://doi.org/10.5194/bg-12-6955-2015>
- Le Grix, N., Zscheischler, J., Laufkötter, C., Rousseaux, C. S., & Frölicher, T. L. (2021). Compound high-temperature and low-chlorophyll extremes in the ocean over the satellite period. *Biogeosciences*, 18(6), 2119–2137. <https://doi.org/10.5194/bg-18-2119-2021>
- Longhurst, A. (1995). Seasonal cycles of pelagic production and consumption. *Progress in Oceanography*, 36(2), 77–167. [https://doi.org/10.1016/0079-6611\(95\)00015-1](https://doi.org/10.1016/0079-6611(95)00015-1)
- Maritorena, S., d'Andon, O. H. F., Mangin, A., & Siegel, D. A. (2010). Merged satellite ocean color data products using a bio-optical model: Characteristics, benefits and issues. *Remote Sensing of Environment*, 114(8), 1791–1804. <https://doi.org/10.1016/j.rse.2010.04.002>
- Martínez-Vicente, V., Evers-King, H., Roy, S., Kostadinov, T. S., Tarran, G. A., Graff, J. R., et al. (2017). Intercomparison of ocean color algorithms for picophytoplankton carbon in the ocean. *Frontiers in Marine Science*, 4, 378. <https://doi.org/10.3389/fmars.2017.00378>
- McClain, C. R. (2009). A decade of satellite ocean color observations. *Annual Review of Marine Science*, 1, 19–42. <https://doi.org/10.1146/annurev.marine.010908.163650>
- Mélin, F. (2016). Impact of inter-mission differences and drifts on chlorophyll-a trend estimates. *International Journal of Remote Sensing*, 37(10), 2233–2251. <https://doi.org/10.1080/01431161.2016.1168949>
- Mélin, F., Vantrepotte, V., Chuprin, A., Grant, M., Jackson, T., & Sathyendranath, S. (2017). Assessing the fitness-for-purpose of satellite multi-mission ocean color climate data records: A protocol applied to OC-CCI chlorophyll-a data. *Remote Sensing of Environment*, 203, 139–151. <https://doi.org/10.1016/j.rse.2017.03.039>
- Moore, C., Mills, M., Arriago, K., Berman-Frank, I., Bopp, L., Boyd, P., et al. (2013). Processes and patterns of oceanic nutrient limitation. *Nature Geoscience*, 6(9), 701–710. <https://doi.org/10.1038/ngeo1765>
- Rodgers, K. B., Lee, S.-S., Rosenbloom, N., Timmermann, A., Danabasoglu, G., Deser, C., et al. (2021). Ubiquity of human-induced changes in climate variability. *Earth System Dynamics*, 12(4), 1393–1411. <https://doi.org/10.5194/esd-12-1393-2021>
- Sankarasubramanian, A., & Lall, U. (2003). Flood quantiles in a changing climate: Seasonal forecasts and causal relations. *Water Resources Research*, 39(5). <https://doi.org/10.1029/2002wr001593>
- Sarmiento, J. L., Slater, R., Barber, R., Bopp, L., Doney, S., Hirst, A., et al. (2004). Response of ocean ecosystems to climate warming. *Global Biogeochemical Cycles*, 18(3), GB3003. <https://doi.org/10.1029/2003gb002134>
- Sathyendranath, S., Brewin, R. J., Brockmann, C., Brotas, V., Calton, B., Chuprin, A., et al. (2019). An ocean-colour time series for use in climate studies: The experience of the ocean-colour climate change initiative (OC-CCI). *Sensors*, 19(19), 4285. <https://doi.org/10.3390/s19194285>
- Sathyendranath, S., Brewin, R. J., Jackson, T., Mélin, F., & Platt, T. (2017). Ocean-colour products for climate-change studies: What are their ideal characteristics? *Remote Sensing of Environment*, 203, 125–138. <https://doi.org/10.1016/j.rse.2017.04.017>
- Sathyendranath, S., Jackson, T., Brockmann, C., Brotas, V., Calton, B., Chuprin, A., et al. (2021). ESA ocean colour climate change initiative (ocean colour CCI): Version 5.0 data [Dataset]. *NERC EDS Centre for Environmental Data Analysis*. <https://doi.org/10.5285/1db7a109c0244aad713e078fd3059a>
- Saulquin, B., Fablet, R., Mangin, A., Mercier, G., Antoine, D., & Fanton d'Andon, O. (2013). Detection of linear trends in multisensor time series in the presence of autocorrelated noise: Application to the chlorophyll-a SeaWiFS and MERIS data sets and extrapolation to the incoming sentinel 3-OLCI mission. *Journal of Geophysical Research: Oceans*, 118(8), 3752–3763. <https://doi.org/10.1002/jgrc.20264>
- Tareghian, R., & Rasmussen, P. (2013). Analysis of arctic and Antarctic sea ice extent using quantile regression. *International Journal of Climatology*, 33(5), 1079–1086. <https://doi.org/10.1002/joc.3491>
- Thomalla, S. J., Nicholson, S.-A., Ryan-Keogh, T. J., & Smith, M. E. (2023). Widespread changes in southern ocean phytoplankton blooms linked to climate drivers. *Nature Climate Change*, 13(9), 1–10. <https://doi.org/10.1038/s41558-023-01768-4>
- Van Oostende, N., Dussin, R., Stock, C., Barton, A., Curchitser, E., Dunne, J. P., & Ward, B. (2018). Simulating the ocean's chlorophyll dynamic range from coastal upwelling to oligotrophy. *Progress in Oceanography*, 168, 232–247. <https://doi.org/10.1016/j.pocean.2018.10.009>
- Vantrepotte, V., & Mélin, F. (2009). Temporal variability of 10-year global SeaWiFS time-series of phytoplankton chlorophyll a concentration. *ICES Journal of Marine Science*, 66(7), 1547–1556. <https://doi.org/10.1093/icesjms/fsp107>
- Westberry, T. K., Schultz, P., Behrenfeld, M. J., Dunne, J. P., Hiscock, M. R., Maritorena, S., et al. (2016). Annual cycles of phytoplankton biomass in the subarctic Atlantic and Pacific Ocean. *Global Biogeochemical Cycles*, 30(2), 175–190. <https://doi.org/10.1002/2015gb005276>
- WMO. (2018). *Guide to climatological practices*. World Meteorological Organization.
- Woolway, R. I., Kraemer, B. M., Zscheischler, J., & Albergel, C. (2021). Compound hot temperature and high chlorophyll extreme events in global lakes. *Environmental Research Letters*, 16(12), 124066. <https://doi.org/10.1088/1748-9326/ac3d5a>
- Yu, S., Bai, Y., He, X., Gong, F., & Li, T. (2023). A new merged dataset of global ocean chlorophyll-a concentration for better trend detection. *Frontiers in Marine Science*, 10, 1051619. <https://doi.org/10.3389/fmars.2023.1051619>
- Zhai, D. (2023). Donggranzhai: Quantile regression for CHL detection: Initial update (v0.1.1) [Software]. *Zenodo*. <https://doi.org/10.5281/zenodo.8343435>
- Zhai, L., Platt, T., Tang, C., Sathyendranath, S., & Walne, A. (2013). The response of phytoplankton to climate variability associated with the North Atlantic oscillation. *Deep Sea Research Part II: Topical Studies in Oceanography*, 93, 159–168. <https://doi.org/10.1016/j.dsr2.2013.04.009>
- Zibordi, G., Voss, K., Johnson, B., & Mueller, J. (2019). *Protocols for Satellite Ocean color data validation: In situ optical radiometry*. IOCCG Protocols Document.